

Quantum Ring in Gapped Graphene Layer with Wedge Disclination in the Presence of an Uniform Magnetic Field

José Amaro Neto, J. R. de S. Oliveira, Claudio Furtado and Sergei Sergeenkov

*Departamento de Física, Universidade Federal da Paraíba,
Caixa Postal 5008, 58051-970, João Pessoa, PB, Brazil.*

Abstract

In this paper we investigate the relativistic quantum dynamics of a massive excitation in a graphene layer with a wedge disclination in the presence of an uniform magnetic field. We use a Dirac oscillator type coupling to introduce the confining potential for massive fermions in this system. We obtain the energy spectrum and eigenfunctions for the quantum ring pierced by Aharonov-Bohm flux resulting in appearance of persistent current and spontaneous magnetization.

PACS numbers: 73.22.-f, 71.55.-i, 03.65.Ge

Keywords: Topological defects, Dirac oscillator, graphene, quantum ring, Magnetization

I. INTRODUCTION

In recent years, some important and interesting physical properties of quantum dots in graphene under the influence of applied magnetic field have attracted much attention [1, 2]. Among numerous theoretical studies, it is worthwhile to mention recent results on different properties of quasiparticles confined in nanostructures, including quantum dots [3, 4] and quantum rings [5–7]. In particular, it was demonstrated that electronic structure, magnetic and transport properties can be significantly altered for graphene in the presence of disclinations. Of special interest is the low-energy behavior of quasiparticles in graphene. At low energies, the quantum behavior of excitations in graphene is described by an equation analogue to a massless Dirac equation [8, 9]. In the absence of a sublattice symmetry, a gap appears and the corresponding dynamics can be incorporated into a massive term in the Dirac equation. It is a known fact that a band gap is induced in these samples, and massive Dirac fermions play a central role in the low-energy limit [10]. It was observed [10] that a substrate induced potential can break the chiral symmetry existing in graphene and, in this way, introduce a mass term in the spectrum of quasiparticles in graphene. In general, this case is called gapped graphene. Recently [11–14], it was demonstrated that the presence of impurities breaks partially the symmetries of the honeycomb lattice in graphene and generates a Dirac mass for the excitations in this material. In this way, the excitations in the gapped graphene are described by a massive Dirac equation. Several studies on the influence of various impurities, electron-electron interactions and substrate structures responsible for appearance of a mass gap in graphene have been carried out [15–25]. These effects imply breaking of sublattice symmetry leading to a mass gap in a graphene layer.

The Hamiltonian describing the π orbitals in a gapped graphene is given by

$$\mathcal{H} = t \sum_{i=A} \sum_{j=1}^3 \left[a^\dagger(\vec{r}_i) b(\vec{r}_i + \vec{u}_j) + b^\dagger(\vec{r}_i + \vec{u}_j) a(\vec{r}_i) \right] + \beta \sum_{i=A} \left[a^\dagger(\vec{r}_i) a(\vec{r}_i) - b^\dagger(\vec{r}_i + \vec{u}_j) b(\vec{r}_i + \vec{u}_j) \right], \quad (1)$$

where t is the probability of transition by tunneling, and 2β is the energy difference of electrons on sites A and B . For massless graphene $\beta = 0$. The creation and annihilation operators create and annihilate electrons in their respective sublattices, i.e., a and a^\dagger act in the sublattice A , while b and b^\dagger in the sublattice B . The vectors \vec{u}_1 , \vec{u}_2 and \vec{u}_3 connect the sites A to their first neighbors.

We can solve the eigenvalue problem by diagonalizing the matrix inside the sum [26, 27]. The corresponding eigenvalues are:

$$E = \pm \left(\beta^2 + t^2 \left[3 + 2 \cos(\sqrt{3}k_y d) + 4 \cos\left(\frac{3}{2}k_x d\right) \cos\left(\frac{\sqrt{3}}{2}k_y d\right) \right] \right)^{1/2}, \quad (2)$$

where d is the distance between carbon atoms in the lattice. The energy eigenvalues display minima in the corners of the Brillouin zone. In this case the separation between the two bands assumes a minimal value at the corners. Notice that only two of six points of the corners of hexagonal Brillouin zone are inequivalent. Therefore, these two points are threefold degenerate. This degeneracy occurs at six points located at the vertices of the first Brillouin zone in the form of a hexagon. Each of them forms, separately, the Fermi surface of graphene, and therefore they are called the Fermi points. In the present case these six points are reduced to only two, which we call K_+ and K_- .

Now let us consider a continuum approximation for small momenta near K_{\pm} , where electrons are found to show a Dirac-like behavior. In this limit, the Hamiltonian assumes the following form

$$\hat{H} = \int \Psi^\dagger H \Psi d^2 r \quad (3)$$

Here, H is the corresponding one-particle Weyl-Dirac Hamiltonian given by

$$H = (-i\gamma^i \partial_i + \gamma^0 m), \quad (4)$$

where γ^μ are the gamma matrices and the spinor is given by $\Psi^T = (\psi_a, \psi_b, \chi_a, \chi_b)$ with a and b being the indices related to A and B sublattice; the spinors ψ and χ correspond to the K_{\pm} Fermi points.

The role of the mass term in graphene is very important for some electronic applications [29]. From the viewpoint of the quantum field theory, generation of an electron mass or opening of a gap in graphene is protected by three-dimensional version of chiral symmetry. It means that we can not open a gap in this material by simply accounting for radiative corrections. A possibility to open a gap in graphene spectrum based on breaking of the product of time reversal and inversion symmetry under an external magnetic field (or when the two Fermi points are involved in case of the Kekule distortion) have been discussed in Refs. [15–25, 30]. Another possibility based on breaking of the chiral symmetry was considered for the case of Haldane model [31] and Kane-Mele model [16] for topological insulators.

It is well known from theoretical and experimental studies of nanostructures of graphene that for large enough applied magnetic fields B , the magnetic length can be made to be of the order of $\ell = \sqrt{\hbar/eB} \approx 50nm$. This observation allows to show the importance of investigating the influence of a disclination in a quantum ring in a graphene layer, noting that the average size of the disclination in this carbon material is of the order of the interatomic distance between two carbon atoms in this nanostructure. This fact shows that since this defect size is smaller than the magnetic length, it can influence the physical properties for this type of materials (such as quantum Hall effect and other electronic properties), in contrast with common topological defects in which the topological defect is much larger than the magnetic length. In Ref. [32] the authors studied the influence of external magnetic field for a quantum dot in graphene with presence of a topological defect. Recently, the influence of a disclination on Landau levels was investigated [33]. By studying a soft confinement in graphene [34], it was observed that the interaction with the substrate of the quantum dots introduces a gap in graphene.

In this contribution, we study the two-dimensional quantum ring in a massive graphene layer, adopting a model of confining quasiparticle in the ring configuration with the potential proposed in Ref. [35] based on using a Dirac oscillator [36] coupling. The Dirac oscillator is a model for a relativistic harmonic oscillator which in the non-relativistic limit became a harmonic oscillator with a strong spin-orbit coupling. This confining potential is a relativistic version of the Tan-Inkson confining potential in two-dimensional semiconductor [37]. In the original model [35] two control parameters were used to obtain a harmonic confinement in a two-dimensional ring. In particular, the quantum point limits are obtained when we make one of the parameters to be zero, $a_1 = 0$. In this relativistic model the confining potential is introduced via the coupling with the momentum of quasiparticle similar to Dirac oscillator [36], namely

$$\vec{\mathbf{p}} \rightarrow \vec{\mathbf{p}} + i \left[\frac{\sqrt{2Ma_1}}{r} + \sqrt{2Ma_2}r \right] \gamma^0 \hat{e}_r, \quad (5)$$

where a_1 and a_2 are the characteristic parameters of the model and M is a quasiparticle mass. Now if we consider the limit $a_1 \rightarrow 0$, the harmonic confining potential of the quantum dot is recovered. In the case $a_2 \rightarrow 0$, the relativistic antidot limit is observed. We use this new coupling in a Dirac equation to describe a quantum ring structure in a massive graphene in the low-energy limit. As it was demonstrated in Ref. [35], the nonrelativistic limit of the

confining model (5) reproduces the quantum ring with confining potential proposed by Tan and Inkson [37]. The Dirac oscillator coupling was used in several applications for graphene [38–43]. Recently, two of us [44] have employed the model proposed in Ref. [35] for the confining potential and investigated the quantum ring in a graphene layer with the presence of a disclination.

In what follows, we study, in low energy limit, the system described by a massive Dirac equation, where a continuous description near Fermi K -points is employed. We use the Dirac oscillator type coupling to confine harmonically the quasiparticles in a quantum ring pierced by Aharonov-Bohm flux in a disclinated massive graphene layer submitted to an uniform magnetic field. We obtain the eigenvalues and eigenfunctions which are used to construct the persistent current. In the case of dynamics in the presence of defects, we demonstrate the dependence of these physical quantities on the parameter characterizing the disclination in a quantum ring.

This paper is organized as follows. In Section II, we study the quantum dynamics of a quasiparticle in a quantum ring in massive graphene layer in the presence of an uniform magnetic field. In Section III, we obtain the persistent current in the studied system. In Section IV, we discuss spontaneous magnetization and its dependence at zero temperature. And finally, in Section V we present our conclusions.

II. QUANTUM RING IN A MASSIVE GRAPHENE LAYER WITH DISCLINATIONS IN THE PRESENCE OF A MAGNETIC FIELD

We can obtain a disclination in a graphene layer by a procedure known as Volterra process [45]. This transformation can be represented by a cut and glue process where we are cutting and removing/adding a sector in a graphene layer, and the resulting disclination is obtained gluing the new edges of the lips. Due to the symmetry of graphene honeycomb lattice the removed or added angular sector must be a multiple of $\pi/3$. We can introduce a topological defect in a graphene layer by a fictitious gauge field following the approach introduced in Refs. [26, 27, 46–49], where a gauge field is introduced in Dirac equation in order to reproduce the already known effect of the disclination on the behavior of the spinor [46, 48]. In this way we can describe the quantum dynamics of a quasiparticle in a gapped graphene layer with a disclination by Dirac equation in curved space in the presence of a non-Abelian

gauge field A_μ^\pm related with K -spin flux. This non-Abelian gauge field is the contribution in the Dirac equation responsible for mixing of points K_\pm [46, 49]. In this way the quantum dynamics of quasiparticles is described by a Dirac equation in a curved background given by following metric

$$ds^2 = dt^2 - dr^2 - \alpha^2 r^2 d\varphi^2 \quad (6)$$

where α is the strength of the disclination which can be written in terms of the angular sector λ which we removed or inserted in the graphene layer to form the defect, as $\alpha = 1 \pm \frac{\lambda}{2\pi}$, where in graphene lattice $\lambda \propto \pi/3$ due to the hexagonal symmetry, so, we have $\lambda = \pm \frac{N\pi}{3}$, where $N \in [0, 6]$ is the number of sectors removed (‘-’) or added (‘+’), that is, positive and negative disclination. A topological defect in a graphene layer of a disclination type is described by the line element (6) corresponding to removed sectors or inserted sectors in this honeycomb lattice, the metric (6) is a continuous description of space with removed/inserted angular sector with a cone geometry. The presence of a disclination in graphene layer can be demonstrated in terms of fluxes of fictitious gauge fields through the apex of the graphene cone. We need two quantum fluxes to describe the presence of disclination in this medium. The first of these quantum fluxes measures the angular deficit of the cone when a spinor is parallel transported around the apex in a closed path proving thus the variation of the local reference frame along the path. The flux produced by this geometric contribution acts only on A/B sublattices and can be determined by using a holonomy transformation [46, 48, 50], that is

$$\oint \Gamma_\mu dx^\mu = \pi(\alpha - 1)\sigma^z \otimes 1. \quad (7)$$

The second quantum flux is called the K -spin flux, and it describes the mixing of the Fermi points K_+ and K_- [49]. This quantum flux can be written in term of the parameter α as

$$\oint A_\mu^\pm dx^\mu = -3\pi(\alpha - 1)1 \otimes \tau^y. \quad (8)$$

It is important to note that τ^i are the Pauli matrices acting only on the K_\pm space. The (8) is the flux associated to a non-Abelian gauge field A_μ^\pm [46, 48, 49]. The introduction of the defect implements a fictitious discontinuity: when a spinor is transported around the apex of disclinated graphene by a closed path of 2π it is forced at some point to jump from a site B to a site B instead of a site A in the sublattices of graphene. This discontinuity is rectified by introducing a non-Abelian vector potential A_μ^\pm term (8) that makes the theory consistent.

This contribution is similar to the Aharonov-Bohm effect for a non-Abelian gauge field. The defect is induced by the presence of an effective curvature in the structure of graphene, in this way both expressions (7) and (8) are functions of the parameter α that characterizes the presence of a disclination. Note that, the non-trivial holonomy introduced by phases (7) is characterized in the Dirac-Weyl equation by spinor connection and it is introduced in the Hamiltonian (4) due to curved space description where usual derivative is changed by the covariant derivative $\partial_\mu \longrightarrow \partial_\mu - \Gamma_\mu$. The effect of the holonomy (8) yields a phase given by [26, 27]

$$\psi(r, \varphi + 2\pi) = e^{i2\pi \left[\pm \frac{3(\alpha-1)1 \otimes \tau^y}{2} \right]} \psi(r, \varphi), \quad (9)$$

and is introduced by a fictitious non-Abelian gauge field, $A_\mu^\pm = \pm \frac{3(\alpha-1)1 \otimes \tau^y}{2r} \hat{e}_\varphi$ in the Hamiltonian of the problem. The effective transport of the Dirac spinor around the apex corresponds to a holonomy transformation for an arbitrary n -disclination and represents a non-Abelian Aharonov-Bohm effect due to presence of topological defect.

In the present paper we have followed the model used in the papers [33, 42, 48, 52], where the influence of disclination is included in two contributions: the first one arises from the description of the Hamiltonian (4) in curved space, in this way the contributions arisen due to holonomy (7) are introduced. The second contribution arising due to the disclination is introduced via a coupling with a non-Abelian field and is present due to the holonomy (8). The confining potential is implemented via minimal coupling in similar way as in a Dirac oscillator. The external magnetic field is introduced by a minimal coupling and has two contributions: one due to the Aharonov-Bohm flux in the center of the ring, and the other due to an uniform magnetic field in the ring.

Now let us define Dirac matrices representation used in this paper. We can build the following 4×4 representation of Dirac matrices in $(2+1)$ -dimensional space using the 2×2 τ^i and σ^i Pauli matrices acting on the Fermi points K_\pm and the sublattices labels A/B , respectively:

$$\begin{aligned} \gamma^0 = \hat{\beta} = \tau^3 \otimes I &= \begin{pmatrix} I & 0 \\ 0 & -I \end{pmatrix}, & \gamma^i = \hat{\beta} \hat{\alpha}^i = i\tau^2 \otimes (\sigma^i) &= \begin{pmatrix} 0 & \sigma^i \\ -\sigma^i & 0 \end{pmatrix}, \\ \hat{\alpha}_i &= \begin{pmatrix} 0 & \sigma^i \\ \sigma^i & 0 \end{pmatrix}, & \Sigma^i &= \begin{pmatrix} \sigma^i & 0 \\ 0 & \sigma^i \end{pmatrix}, \end{aligned} \quad (10)$$

with $(i = 1, 2, 3)$. I and σ^i stand for 2×2 the identity matrix and Pauli matrices respectively

and $\vec{\Sigma}$ being the spin vector. The matrices $\hat{\alpha}^i (i = 1, 2, 3)$ and $\hat{\beta}$ satisfy the set of properties: $\hat{\alpha}^i \hat{\alpha}^j + \hat{\alpha}^j \hat{\alpha}^i = 2\delta_{ij}I$, $\hat{\alpha}^i \hat{\beta} = -\hat{\beta} \hat{\alpha}^i$ and $\hat{\alpha}^{i2} = \hat{\beta}^2 = I$. Note that we have used a Dirac-Pauli representation of Dirac matrices [28]. Now we can write the Dirac equation associated to Hamiltonian (4) for gapped graphene with a disclination (in a curved space (6)) and considering the presence of non-Abelian gauge field (8) due to the presence of topological defect under the influence of external magnetic fields and a confinement potential due to a quantum ring. The result is as follows

$$\left(i\gamma^\mu \frac{\partial}{\partial x^\mu} - i\gamma^\mu \Gamma_\mu + \gamma^\mu \mathbf{A}_\mu^C - \gamma^\mu e \mathbf{A}_\mu - \gamma^\mu \mathbf{A}_\mu^\pm \right) \Psi = M\Psi. \quad (11)$$

with γ^μ being the Dirac matrices defined in a curved space. The Γ_μ term is a spinor connection which is present due to the curved nature of the geometry of the disclinated gapped graphene lattice in an elastic continuous limit (6). The matrices γ^μ in a curved space can be expressed as functions of triad fields $e_a^\mu(x)$. In this curved background frame, the Dirac matrices must be defined by $\gamma^\mu = e_a^\mu(x)\gamma^a$ and satisfy the anticommutation relation $\{\gamma^a, \gamma^b\} = 2\eta^{ab}$, where η^{ab} the usual Minkowski metric with a signature $\eta^{ab} = \text{diag}(+, -, -)$. The γ^μ matrices are related to the γ^a matrices via $\gamma^\mu = e_a^\mu(x)\gamma^a$. Moreover, the *vierbein fields* satisfy the relation $g^{\mu\nu} = e_a^\mu e_b^\nu \eta^{ab}$. So that we can write the triad matrix e_a^μ and its inverse e_a^μ as

$$e_a^\mu = \begin{pmatrix} 1 & 0 & 0 \\ 0 & \cos \varphi & -\alpha r \sin \varphi \\ 0 & \sin \varphi & \alpha r \cos \varphi \end{pmatrix}, \quad e_a^\mu = \begin{pmatrix} 1 & 0 & 0 \\ 0 & \cos \varphi & \sin \varphi \\ 0 & -\frac{\sin \varphi}{\alpha r} & \frac{\cos \varphi}{\alpha r} \end{pmatrix}. \quad (12)$$

From matrices (12), we can obtain the 1-form of connection ω_b^a through the Maurer-Cartan structure equation $de^a + \omega_b^a \wedge e^b = 0$ (without torsion). Due to the symmetry of the defect, the connections have only two non-zero components, $\omega_1^2 = -\omega_2^1 = -(\alpha - 1)d\varphi$. In this way, the spinorial connection is described in terms of the spin connection, by the equation $\Gamma_\mu = \frac{i}{4}\omega_{\mu ab}\Sigma^{ab}$ such that $\Sigma^{ab} = \frac{i}{2}(\gamma^a\gamma^b - \gamma^b\gamma^a)$. Hence, the only non-zero spinorial connection component is:

$$\Gamma_\varphi = -\frac{i}{2}(\alpha - 1)\Sigma^3. \quad (13)$$

The terms contained in Dirac equation have the following origin: the term Γ_μ is the spinorial connection arisen due to the change in the geometry of graphene introduced by disclination. It is responsible for a non-trivial holonomy due to the parallel transport of spinor (7) in

the geometry (6), and for the variation of the local reference frame in this geometry, and produces a geometric phase that acts in the sublattices A/B of graphene [46, 48]. The second term \mathbf{A}_μ^C is the confinement potential given by (5). We note the presence of the term $A_\mu^\pm = \pm \frac{3}{2r}(\alpha-1)1 \otimes \tau^2$ due to the non-Abelian gauge field related to the K-spin flux because of the geometric phase (8), and contributing for the mixing of the Fermi points K_\pm . The coupling with the potential vector \mathbf{A}_μ is responsible for the inclusion of the Aharonov-Bohm flux[51] piercing through the center of the quantum ring and an uniform magnetic field in the z -direction, given by

$$\vec{\mathbf{A}} = \left[\frac{\Phi}{2\pi r} + \frac{Br}{2\alpha} \right] \hat{e}_\varphi, \quad (14)$$

where the first contribution $\frac{\Phi}{2\pi r}$ arises due to the Aharonov-Bohm flux in center of the quantum ring, and the second contribution $\frac{Br}{2\alpha}$ is due to an uniform magnetic field in the ring with topological defect in the similar way to Tan-Inkson model [37, 53, 54] for metallic/semiconductor quantum ring. Now, using the triads (12), we obtain the following equation

$$\begin{aligned} & \left[i\gamma^t \frac{\partial}{\partial t} + i\gamma^r \left(\frac{\partial}{\partial r} - \left[\frac{\sqrt{2Ma_1}}{r} - \sqrt{2Ma_2}r \right] \gamma^0 + \frac{(\alpha-1)}{2\alpha r} \right) \right] \Psi \\ & + \left[i\gamma^\varphi \left(\frac{1}{\alpha r} \frac{\partial}{\partial \varphi} + i\frac{\phi_{AB}}{r} + i\frac{eBr}{2\alpha} + i\frac{a_\varphi}{r} \right) \right] \Psi = M\Psi, \end{aligned} \quad (15)$$

with $a_\mu = \pm \frac{3}{2}(\alpha-1)$, $\phi_{AB} = \frac{\Phi}{\Phi_0}$ and $\Phi_0 = \frac{2\pi}{e}$ is the quantum of the magnetic flux. The spin connection is responsible by following term in (15) $\gamma^\varphi \Gamma_\varphi = \frac{(\alpha-1)}{2\alpha r}$. We assume the gamma matrices in curved background (6) to be given by:

$$\gamma^\mu = e_a^\mu \gamma^a = \begin{cases} \bar{\gamma}^0 = \gamma^0 = \gamma^t; \\ \bar{\gamma}^1 = \gamma^1 \cos\varphi + \gamma^2 \sin\varphi = \gamma^r; \\ \bar{\gamma}^2 = -\frac{\gamma^1}{\alpha r} \sin\varphi + \frac{\gamma^2}{\alpha r} \cos\varphi = \frac{\gamma^\varphi}{\alpha r}. \end{cases} \quad (16)$$

From (15), using the gamma matrices (10) we can rewrite the effective Hamiltonian for this system in the following form

$$\begin{aligned}
H = & -i\hat{\alpha}^r \left(\frac{\partial}{\partial r} - \left[\frac{\sqrt{2Ma_1}}{r} - \sqrt{2Ma_2r} \right] \hat{\beta} + \frac{(\alpha-1)}{2\alpha r} \right) \\
& -i\hat{\alpha}^\varphi \left(\frac{1}{\alpha r} \frac{\partial}{\partial \varphi} + i\frac{\phi_{AB}}{r} + i\frac{eBr}{2\alpha} + i\frac{a_\varphi}{r} \right) + \hat{\beta}M,
\end{aligned} \tag{17}$$

where we define $a_\varphi = \pm \frac{3}{2}(\alpha-1)$. Now the Dirac equation is given by $H\Psi = E\Psi$. Splitting this equation into two decoupled equations is well known in the massless case [8, 9, 46, 50] but this is possible also in some situations in a massive case [27, 55, 56]. In the present case a transformation cannot be defined from results for an effective Abelian gauge field. In this way we use the non-Abelian phase (9) in the construction of the effective Hamiltonian. We use a similarity transformation to eliminate the contribution arisen due to the spinorial connection in the Dirac equation (15) [57]. We choose the following similarity transformation $S(\varphi) = e^{-i\frac{\varphi}{2}\Sigma^3}$ to change the representation of local Dirac matrices, $(\gamma^r, \gamma^\varphi) = \bar{\gamma}^j$. Thus, we write the Ansatz for Ψ' given by

$$\Psi' = e^{-iEt - i\frac{\varphi}{2}\Sigma^3} \begin{pmatrix} \psi(r, \varphi) \\ \chi(r, \varphi) \end{pmatrix} \tag{18}$$

where, as it was mentioned above, $\psi = \psi(r, \varphi)$ and $\chi = \chi(r, \varphi)$ represent the sublattices A and B respectively. From the similarity transformations and Ansatz (18), we obtain the set of equations:

$$\begin{aligned}
(E - M)\psi = & -i\sigma^1 \left[\frac{\partial}{\partial r} + \frac{1}{2r} + \frac{\sqrt{2Ma_1}}{r} + \sqrt{2Ma_2r} \right] \chi \\
& -i\sigma^2 \left[\frac{1}{\alpha r} \frac{\partial}{\partial \varphi} + \frac{i\phi_{AB}}{r} + \frac{ieBr}{2\alpha} + \frac{ia_\varphi}{r} \right] \chi
\end{aligned} \tag{19}$$

and

$$\begin{aligned}
(E + M)\chi = & -i\sigma^1 \left[\frac{\partial}{\partial r} + \frac{1}{2r} - \frac{\sqrt{2Ma_1}}{r} - \sqrt{2Ma_2r} \right] \psi \\
& -i\sigma^2 \left[\frac{1}{\alpha r} \frac{\partial}{\partial \varphi} + \frac{i\phi_{AB}}{r} + \frac{ieBr}{2\alpha} + \frac{ia_\varphi}{r} \right] \psi.
\end{aligned} \tag{20}$$

Now, we eliminate the χ in (19) substituting (20) into it, and obtain the following second-

order differential equation:

$$\begin{aligned}
(E^2 - M^2)\psi = & -\frac{\partial^2 \psi}{\partial r^2} - \frac{1}{r} \frac{\partial \psi}{\partial r} + \frac{\psi}{4r^2} - \frac{\sqrt{2Ma_1}}{r^2} \psi + \sqrt{2Ma_2} \psi + \frac{2Ma_1}{r^2} \psi + 2Ma_2 r^2 \psi + \\
& + 4M\sqrt{a_1 a_2} \psi - \frac{1}{\alpha^2 r^2} \frac{\partial^2 \psi}{\partial \varphi^2} + i \frac{\sigma^3}{\alpha r^2} \frac{\partial \psi}{\partial \varphi} - 2i\sigma^3 \frac{\sqrt{2Ma_1}}{\alpha r^2} \frac{\partial \psi}{\partial \varphi} - \frac{2i\sigma^3 \sqrt{2Ma_2}}{\alpha} \frac{\partial \psi}{\partial \varphi} - \\
& - 2i \frac{\phi_{AB}}{\alpha r^2} \frac{\partial \psi}{\partial \varphi} - \frac{iBe}{\alpha^2} \frac{\partial \psi}{\partial \varphi} - \frac{2ia_\varphi}{\alpha r^2} \frac{\partial \psi}{\partial \varphi} \\
& + 2eB\sigma^3 \frac{\sqrt{2Ma_1}}{2\alpha} \psi + 2\sigma^3 a_\varphi \frac{\sqrt{2Ma_1}}{r^2} \psi + 2\sigma^3 \phi_{AB} \frac{\sqrt{2Ma_1}}{r^2} \psi + 2\sigma^3 \phi_{AB} \sqrt{2Ma_2} \psi \\
& + 2eB\sigma^3 \frac{\sqrt{2Ma_2} r^2}{2\alpha} \psi + 2\sigma^3 \sqrt{2Ma_2} a_\varphi \psi + \sigma^3 \frac{eB}{2\alpha} \psi - \sigma^3 \frac{a_\varphi}{r^2} \psi - \sigma^3 \frac{\phi_{AB}}{r^2} \psi \\
& + \frac{\phi_{AB}^2}{r^2} \psi + 2eB \frac{\phi_{AB}}{2\alpha} \psi + \frac{a_\varphi^2}{r^2} \psi + \frac{2\phi_{AB} a_\varphi}{r^2} \psi + 2eB \frac{a_\varphi}{2\alpha} \psi + \frac{e^2 B^2 r^2}{4\alpha^2} \psi. \quad (21)
\end{aligned}$$

Then, to obtain the solution of the Eq.(21), we make the following choice for the function ψ :

$$\psi(r, \varphi) = e^{im\varphi} \begin{pmatrix} R_+(r) \\ R_-(r) \end{pmatrix} = e^{im\varphi} R_s(r), \quad (22)$$

where $m = l + \frac{1}{2}$, is semi-integer with $l = 0, \pm 1, \pm 2, \dots$ and $R_s = (R_+(r), R_-(r))$. In this way we obtain the following set of equations

$$\left[\frac{d^2}{dr^2} + \frac{1}{r} \frac{d}{dr} - \frac{\delta_s^2}{\alpha^2 r^2} - \frac{\omega_\alpha^2 M^2}{4} r^2 + \epsilon_s \right] R_s(r) = 0, \quad (23)$$

with parameters δ_s , ϑ_s , ϵ_s and ω_α defined as:

$$\begin{aligned}
\delta_s &= \vartheta_s + \alpha s \sqrt{2Ma_1}, \\
\vartheta_s &= (l + \alpha \phi_{AB}) + \frac{(1 - \alpha s)}{2} + \alpha a_\varphi, \\
\epsilon_s &= E^2 - M^2 - M \frac{(\delta_s + \alpha s)}{\alpha} \left(\omega_0 s + \frac{\omega_c}{\alpha} \right), \\
\omega_\alpha &= \sqrt{\omega_0^2 + \frac{2\omega_0 \omega_c s}{\alpha} + \frac{\omega_c^2}{\alpha^2}} \quad (24)
\end{aligned}$$

with $\omega_0 = \sqrt{\frac{8a_2}{M}}$ being the characteristic frequency and $\omega_c = \frac{eB}{M}$ is the cyclotron frequency.

To solve the equation (23) we make the change of the variable $\rho = \sqrt{\frac{\omega_\alpha^2 M^2}{4}} r^2$ so that afterwards our equation takes the form:

$$\left[\rho \frac{d^2}{d\rho^2} + \frac{d}{d\rho} - \frac{\delta_s^2}{4\alpha^2 \rho} - \frac{\rho}{4} + \frac{\epsilon_s}{2M\omega_\alpha} \right] R_s(\rho) = 0. \quad (25)$$

In this way, we do the asymptotic analysis of Eq. (23), for the limits $R_s \rightarrow 0$ and $r \rightarrow \infty$, it is possible to present radial equation in the following form:

$$R_s(\rho) = e^{\frac{-\rho}{2}} \rho^{\frac{|\delta_s|}{2\alpha}} F_s(\rho) \quad (26)$$

Substituting this into the previous equation we obtain:

$$\rho \frac{d^2 F_s(\rho)}{d\rho^2} + \left[\frac{|\delta_s|}{\alpha} + 1 - \rho \right] \frac{dF_s(\rho)}{d\rho} + \left[\frac{\epsilon_s}{2M\omega_\alpha} - \frac{|\delta_s|}{2\alpha} - \frac{1}{2} \right] F_s(\rho) = 0, \quad (27)$$

where Eq. (27) is the hypergeometric equation whose solution is the hypergeometric function:

$$F_s(\rho) = {}_1F_1(a, b; z) = {}_1F_1 \left(\frac{|\delta_s|}{2\alpha} + \frac{1}{2} - \frac{\epsilon_s}{2M\omega_\alpha}, \frac{|\delta_s|}{\alpha} + 1, \rho \right). \quad (28)$$

Now to get a finite solution anywhere, we impose the condition that the solution of hypergeometric series becomes a polynomial of degree n , that is: $\frac{|\delta_s|}{2\alpha} + \frac{1}{2} - \frac{\epsilon_s}{2M\omega_\alpha} = -n$ from this equation, substituting the parameters (24), we obtain the energy spectrum for the particle confined in two-dimensional quantum ring pierced by Aharonov-Bohm quantum flux in gapped graphene in the presence of the uniform magnetic field:

$$E_{n,l}^2 = \left(2n + \frac{|\delta_s|}{\alpha} + 1 \right) M\omega_\alpha + M \frac{(\delta_s + \alpha s)}{\alpha} \left(\omega_0 s + \frac{\omega_c}{\alpha} \right) + M^2, \quad (29)$$

where $s = +1$ corresponds to sublattice A and $s = -1$ corresponds to sublattice B . Note that the spectrum depends on the quantum numbers n and l , the cyclotron frequency ω_c , and, in addition, on the new frequency related to the topological defect ω_α through the dependence on the parameter α . Note that $\delta_s = (l + \alpha\phi_{AB}) + \frac{(1-\alpha s)}{2} + \alpha a_\varphi + \alpha s \sqrt{2Ma_1}$ where $\phi_{AB} = \frac{\Phi}{\Phi_0}$. This way the eigenvalues of energy (29) are periodic functions of Φ with the period Φ_0 . A similar behaviour was observed for semiconductor quantum ring in Refs.[37, 67]. Moreover, the Eq. (29) has a contribution of the non-Abelian gauge field A_φ^\pm responsible for the Aharonov-Bohm effect of the spinors, due to the presence of the disclination.

Notice that according to Fig. 1, for the positive disclinations the energy eigenvalues have magnitude greater than in the flat case, while in the case of negative disclinations the energy assumes smaller values for the same quantum number n .

The solutions with positive energy describe the dynamics of electrons in the conduction band while negative energy corresponds to the dynamics of holes in the valence band. In this paper we address only the first case. Also, as it was argued earlier, components of the spinor in graphene describe the contributions of sub-lattices, with the real spins of the particles are not considered within this approach. For equation (29), the spinors corresponding to

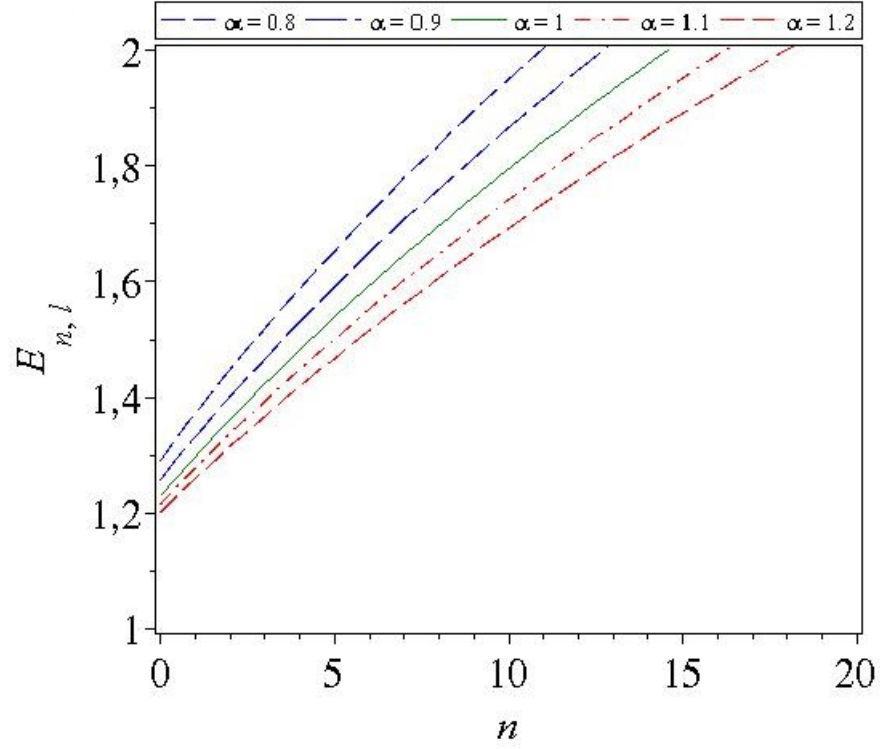


Figure 1. The obtained energy spectrum as a function of quantum number n for several values of α . We have adopted the following values for model parameters: $B = 1T$, $M = 1$, $l = 1$, $\phi_{AB} = 1$, and $s = 1$. $a_1 = 9.0122 \times 10^{-6} eV.m^2$ and $a_2 = 2.222 \times 10^{-5} eV.m^{-2}$ are the Tan -Inkson parameters [37].

positive energy for $s = +1$ and $\eta_-(r) = 0$ are written as:

$$\begin{aligned} \Psi_+ = & f_+ {}_1F_1 \left(-n, \frac{|\delta_+|}{\alpha} + 1, \frac{\omega_\alpha M}{2} r^2 \right) \times \\ & \begin{pmatrix} 1 \\ 0 \\ 0 \\ \frac{i}{E+M} \left[\frac{M}{2} [(\omega_0 + \omega_c/\alpha) + \omega_0] r + \frac{(\vartheta_+ - |\delta_+| + \alpha\sqrt{2Ma_1})}{\alpha r} - \frac{M\omega_c r}{2\alpha} \right] \end{pmatrix} \\ & + \frac{if_+}{E+M} \left(\frac{nM(\omega_0 + \omega_c/\alpha)r}{\frac{|\delta_+|}{\alpha} + 1} \right) {}_1F_1 \left(-n + 1, \frac{|\delta_+|}{\alpha} + 2, \frac{\omega_\alpha M}{2} r^2 \right) \begin{pmatrix} 0 \\ 0 \\ 0 \\ 1 \end{pmatrix}, \end{aligned} \quad (30)$$

and for $s = -1$ and $\eta_+(r) = 0$ as

$$\begin{aligned}
\Psi_- = & f_{-1} F_1 \left(-n, \frac{|\delta_-|}{\alpha} + 1, \frac{\omega_\alpha M}{2} r^2 \right) \times \\
& \begin{pmatrix} 0 \\ 1 \\ \frac{i}{E+M} \left[\frac{M}{2} [(\omega_0 + \omega_c/\alpha) + \omega_0] r - \frac{(\vartheta_- + |\delta_-| - \alpha \sqrt{2Ma_1})}{\alpha r} + \frac{M\omega_c r}{2\alpha} \right] \\ 0 \end{pmatrix} \\
& + \frac{if_-}{E+M} \left(\frac{nM(\omega_0 + \omega_c/\alpha)r}{\frac{|\delta_-|}{\alpha} + 1} \right) {}_1F_1 \left(-n + 1, \frac{|\delta_-|}{\alpha} + 2, \frac{\omega_\alpha M}{2} r^2 \right) \begin{pmatrix} 0 \\ 0 \\ 1 \\ 0 \end{pmatrix}. \quad (31)
\end{aligned}$$

Both in (30) and (31), the factor $f_s = N_s e^{-iEt}$ reads

$$f_s = \left(\frac{M\omega_\alpha \Gamma \left(\frac{|\delta_s|}{\alpha} + n + 1 \right)}{\Gamma(n+1) \left[\Gamma \left(\frac{|\delta_s|}{\alpha} + 1 \right) \right]^2} \right)^{1/2} \times e^{-iEt} e^{i(l+1/2)\varphi} e^{-\frac{\omega_\alpha M}{4} r^2} \left(\frac{\omega_\alpha^2 M^2}{4} \right)^{\frac{|\delta_s|}{4\alpha}} r^{\frac{|\delta_s|}{\alpha}}. \quad (32)$$

Note that at $\alpha = 1$, the non-Abelian gauge field α_ϕ goes to zero and the parameters δ_s , ϑ_s , ϵ_s and ω_α tend to the values of the parameters λ_s , ξ_s , ε_s and ω respectively. In other words, we recover the spectrum, persistent current, and spinors of positive energy for the case of flat sheet without defect, i.e., $\alpha = 1$ represents the absence of topological defect of the gapped graphene layer. Moreover, if we switch off the magnetic field, i.e., make $B = 0$ and by consequence $\omega_c = 0$, we recover the case of a two-dimensional ring in a gapped graphene layer, and in the case $M = 0$ we obtain the results which were considered in Ref. [44].

III. THE PERSISTENT CURRENT IN THE PRESENCE OF A DISCLINATION

The study of small conducting rings pierced by a magnetic flux in low temperature limit predicted the emergence of persistent currents [58] in these systems. This current is a thermodynamic effect deeply connected with the presence of quantum coherence. The theoretically predicted persistent current has been experimentally observed in a ring in several experiments in metals [59–61] and semiconductors [62]. Now let us calculate the persistent

current for our model of quantum ring in a graphene layer with a disclination. The persistent current carried by a given electron state is calculated using the Byers-Yang relation [63]. This relation expresses the persistent current as a derivative of the energy with respect to the magnetic flux

$$I = -\frac{\partial U}{\partial \Phi} = -\sum_{n,l} \frac{\partial E_{n,l}}{\partial \Phi}, \quad (33)$$

where $U = \sum_{n,l} E_{n,l}$ is total energy of system and we consider the zero temperature $T = 0$ and a fixed number of quasiparticles n . The summation is realized over the n occupied states.

In this way, the persistent current for our system reads:

$$I = \left(\frac{\mp e}{4\pi} \right) \sum_{n,l} M \left(\frac{\delta_s}{|\delta_s|} \omega_\alpha + \frac{\omega_c}{\alpha} + s\omega_0 \right) \times \\ \times \left\{ M^2 + M \frac{(\delta_s + \alpha s)}{\alpha} \left(\omega_0 s + \frac{\omega_c}{\alpha} \right) + \left(2n + \frac{|\delta_s|}{\alpha} + 1 \right) M \omega_\alpha \right\}^{-1/2} \quad (34)$$

Note that the persistent current is a function of the parameter characterizing the curved geometry introduced by a topological defect. The expression for the persistent current given by (34) is a function of the non-Abelian magnetic flux and the Aharonov-Bohm flux on which the parameter δ_s depends. The current has jumps with a certain periodicity and is function of the Aharonov-Bohm flux Φ . Fig.2 shows the predicted behavior when the oscillations vanish for the large values of the Aharonov-Bohm flux.

We can compare our results with those obtained for quantum dots in graphene. The predicted here oscillatory behavior turns out to be similar to the one observed in Ref. [33].

IV. THE MAGNETIZATION FOR QUANTUM RING IN PRESENCE OF DISCLINATION

Now, we investigate the magnetization for a quasiparticle in quantum ring in a graphene sheet at zero temperature. In general, an analytic expression for a magnetization μ is defined via applied magnetic field B as follows

$$\mu(B) = -\frac{\partial U}{\partial B} = -\sum_{n,l} \frac{\partial E_{n,l}}{\partial B}, \quad (35)$$

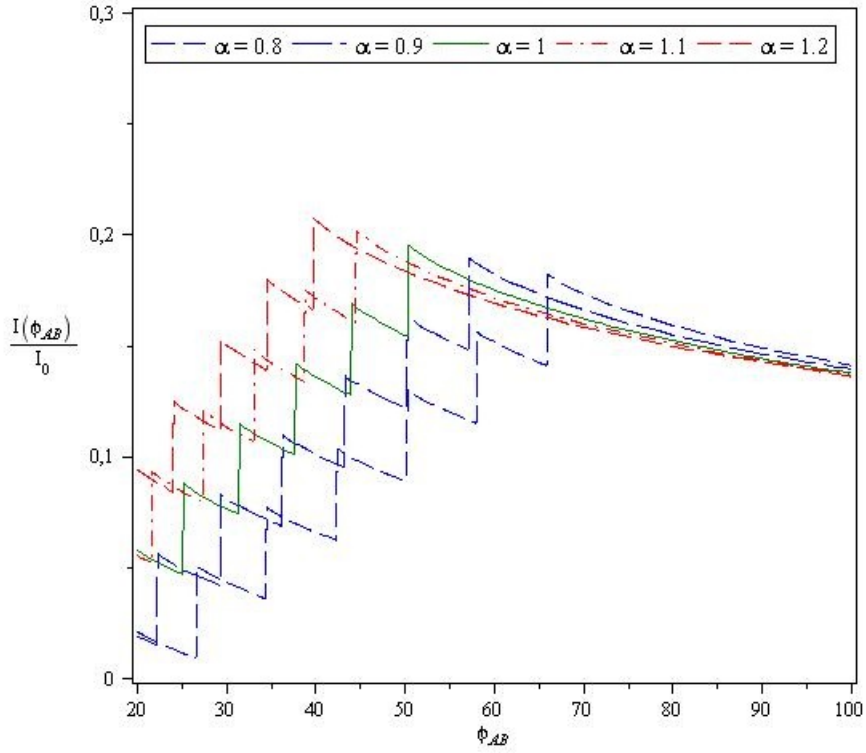


Figure 2. The behavior of persistent current as a function of magnetic flux $\phi_{AB} = \frac{\Phi}{\Phi_0}$ for several values of α . The topological current term is defined as $I_0 = \frac{1}{2\phi_0} \left(\sqrt{\frac{8a_2}{M}} s + \frac{eB}{\alpha M} \right)$. The values for the other parameters are $B = 1T$, $M = 1$, $s = 1$, $-10 \leq l \leq 10$ and $0 \leq n \leq 5$. $a_1 = 9.0122 \times 10^{-6} eV.m^2$ and $a_2 = 2.222 \times 10^{-5} eV.m^{-2}$

where we consider a system with a temperature $T = 0$ and a fixed number N of spinless particles and the summation is realized over the N occupied states. Using (29), we obtain:

$$\mu(B, \alpha) = - \sum_{n,l} \left(\frac{se}{2} \right) \left[\frac{\left(2n + \frac{|\delta_s|}{\alpha} + 1 \right)}{\alpha} + \frac{\delta_s + \alpha s}{\alpha^2} \right] \times \quad (36)$$

$$\left\{ M^2 + M \frac{(\delta_s + \alpha s)}{\alpha} \left(\omega_0 s + \frac{\omega_c}{\alpha} \right) + \left(2n + \frac{|\delta_s|}{\alpha} + 1 \right) M \omega_\alpha \right\}^{-1/2}, \quad (37)$$

We can conclude from Eq (37) that the spontaneous zero-field magnetization strongly depends on the parameter α characterizing the presence of disclination in a graphene layer. This dependence is shown in Fig. 3 where $\mu(0, 1)$ corresponds to spontaneous magnetization of the defect-free system with $\alpha = 1$. And finally, Fig.4 depicts field dependence of the

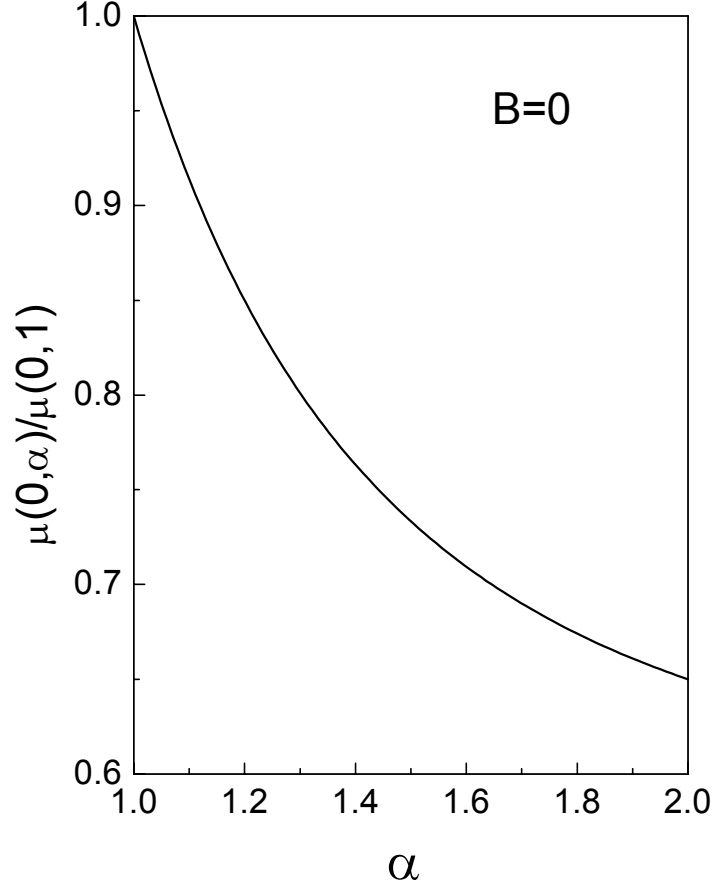


Figure 3. The behavior of normalized zero-field (spontaneous) magnetization as a function of disclination parameter α . In this plot, we used $B = 0$, $M = 1$, $\phi_{AB} = 1$, $s = -1$, $a_1 = 9.0122 \times 10^{-6} \text{eV.m}^2$ and $a_2 = 2.222 \times 10^{-5} \text{eV.m}^{-2}$. The sum runs over $-10 \leq l \leq 10$ and $0 \leq n \leq 5$.

induced magnetization $\mu(B, \alpha)$ for different values of the defect controlling parameter α . Observe that high field magnetization quite markedly increases with the number of defects in the studied system.

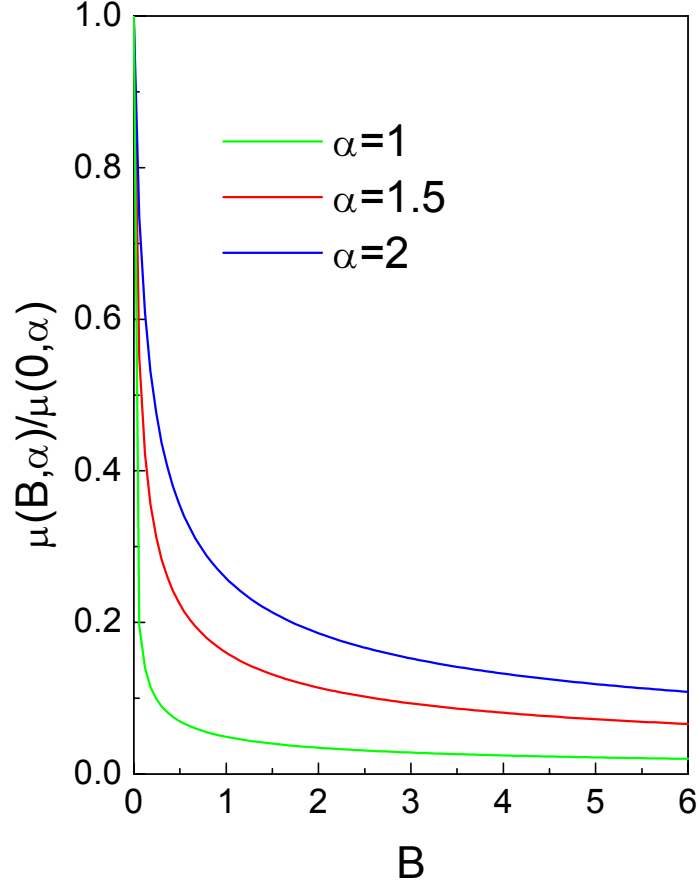


Figure 4. Magnetic field dependence of normalized magnetization for different values of disclination parameter α changing from defect-free value of $\alpha = 1$ (corresponding to $N = 0$) to its maximum number $\alpha = 2$ (corresponding to $N = 6$). In this plot, we used $M = 1$, $\phi_{AB} = 1$, $s = -1$, $a_1 = 9.0122 \times 10^{-6} \text{eV.m}^2$ and $a_2 = 2.222 \times 10^{-5} \text{eV.m}^{-2}$. The sum runs over $-10 \leq l \leq 10$ and $0 \leq n \leq 5$.

V. CONCLUSIONS

In this contribution we have studied a quantum ring in a gapped graphene layer with a topological defect submitted to an uniform magnetic field along z -direction. We use a confinement potential proposed in Ref. [35] to confine a quasiparticle in a two-dimensional

quantum ring. This potential was introduced in Dirac equation using minimal coupling similar to Dirac oscillator. We have considered an Aharonov-Bohm magnetic flux in the center of quantum ring. The quantum dynamics of the massive quasiparticle in the presence of a disclination is determined by a quantum ring potential. The eigenvalues of energy are obtained, and we found that the energy is a periodic function of the Aharonov-Bohm flux Φ with the period Φ_0 . We have demonstrated the influence of the disclination on energy levels. Namely, for a positive disclination the energy eigenvalues increase with growing of parameter of disclination α , while for the case of a negative disclination $\alpha < 1$ eigenvalues of energy decrease in comparison with the case of a gapped graphene layer without a defect. The persistent current, for $T = 0$, was obtained, and its expression turns out to depend on the parameter α characterizing the presence of the disclination. It has jumps with a certain periodicity on the non-Abelian field $a_\varphi = \pm \frac{3}{2}(\alpha - 1)$ and the Aharonov-Bohm $\phi_{AB} = \frac{\Phi}{\Phi_0}$ fluxes. We have also obtained an analytic expression for zero-temperature magnetization and found that it is a periodic function of fluxes. We conclude that the role of geometry introduced by topological defects in the electronic properties of graphene is central for the realization of the future investigation regarding quantum computation in these systems [64–66].

Acknowledgments. We are grateful to Knut Bakke for interesting discussion. We thank CNPq, CAPES, CNPq/Universal and FAPESQ for financial support.

-
- [1] L. A. Ponomarenko, F. Schedin, M. I. Katsnelson, R. Yang, E. W. Hill, K. S. Novoselov, and A. K. Geim, *Science* **320**, 356 (2008).
 - [2] S. Schnez, F. Molitor, C. Stampfer, J. Güttinger, I. Shorubalko, T. Ihn, and K. Ensslin, arXiv: 0807.2710.
 - [3] P. G. Silvestrov and K. B. Efetov, *Phys. Rev. Lett.* **98**, 016802 (2007).
 - [4] S. Schnez, K. Ensslin, M. Sigrist, and T. Ihn, *Phys. Rev. B* **78**, 195427 (2008).
 - [5] M D Petrović, F. M. Peeters, A. Chaves. and G. A. Farias, *J. Phys.: Cond. Mat.* **25** 495301 (2013).
 - [6] M. Grujić, M. Tadić and F. M. Peeters, *Phys Rev. B* **87**, 085434 (2013).

- [7] D. R. da Costa, A. Chaves, M. Zarenia, J. M. Pereira Jr., G. A. Farias, and F. M. Peeters, Phys Rev. B **89**, 075418 (2014).
- [8] J. Gonzalez, F. Guinea, and M. A. H. Vozmediano, Nuclear Physics B **406**, 771 (1993).
- [9] A. H. Castro Neto, F. Guinea, N. M. R. Peres, K. S. Novoselov, and A. K. Geim, Rev. Mod. Phys. **81**, 109 (2009).
- [10] S. Y. Zhou, G.-H. Gweon, A. V. Fedorov, P. N. First, W. A. de Herr, D.-H. Lee, F. Guinea, A. H. Castro Neto and A. Lanzara, Nature Materials **6**, 770 (2007).
- [11] V. R. Khalilov and C. L. Ho, Mod. Phys. Lett. A **13**, 615 (1998).
- [12] D. S. Novikov, Phys. Rev. B **76**, 245435 (2007).
- [13] V. M. Pereira, V. N. Kotov and A. H. Castro Neto, Phys. Rev. B **78**, 085101 (2008).
- [14] V. N. Kotov, V. M. Pereira, B. Uchoa, Phys. Rev. B **78**, 075433 (2008).
- [15] E. V. Gorbar, V. P. Gusynin, V. A. Miransky and I. A. Shovkovy, Phys. Rev. B **66**, 045108 (2002).
- [16] C. L. Kane and E. J. Mele, Phys. Rev. Lett. **95**, 226801 (2005).
- [17] D. S. Novikov, Phys. Rev. B **76**, 245435 (2007).
- [18] D. V. Khveshchenko, J. Phys.: Cond. Mat. **21**, 075303 (2009).
- [19] O. V. Gamayun, E. V. Gorbar and V. P. Gusynin, Phys. Rev. B **81**, 075429 (2010).
- [20] W. Li, G.-Z. Liu, Phys. Lett. A **374**, 2957 (2010).
- [21] Y. Araki and T. Hatsuda, Phys. Rev. B **82**, 121403 (R) (2010).
- [22] M. Y. Han *et al.*, Phys. Rev. Lett. **98**, 206805 (2007).
- [23] S. Y. Zhou *et al.*, Nat. Mater. **7**, 259 (2008).
- [24] D. Haberer *et al.*, Nano Lett. **10**, 3360 (2010).
- [25] D.-K. Ki, A. F. Morpurgo, Phys. Rev. Lett. **108**, 266601 (2012).
- [26] B. Chakraborty, K. S. Gupta and S. Sen, Phys. Rev. B **83**, 115412 (2011).
- [27] J. F. O. de Souza, C. A. de Lima Ribeiro and C. Furtado, Phys. Lett. A **378**, 2317 (2014).
- [28] B. S. Kandemir and A. Mogulkoc, Eur. Phys. J. B **74** 535 (2010).
- [29] A Cortijo, F Guinea and M A H Vozmediano, J. Phys. A: Math. Theor. **45** 383001 (2012).
- [30] J. L. Mañes, F. Guinea, and M. A. H. Vozmediano, Phys. Rev. B **75**, 155424 (2007)
- [31] F. D. M. Haldane, Phys. Rev. Lett. **61**, 2015 (1988).
- [32] D. Akay and B. S. Kandemir, Int Journal of Chemical, Molecular, Nuclear, Materials and Metallurgical Engineering **10**, 54 (2016).

- [33] M. J. Bueno, C. Furtado and A. M. de M. Carvalho, Eur. Phys. J. B **85**, 53 (2012).
- [34] D. Subramaniam, F. Libisch, Y. Li *et al.*, Phys. Rev. Lett. **108**, 046801 (2012).
- [35] K. Bakke, C. Furtado, Phys. Lett. A **376**, 1269 (2012).
- [36] M. Moshinsky and A. Szczepaniak, J. Phys. A: Math. Gen. **22**, 1817 (1989).
- [37] W.-C Tan, J. C. Inkson, Phys. Rev. B **60**, 5626 (1999).
- [38] C. Quimbay, P. Strange, arXiv:1311.2021.
- [39] A. Belouad, A. Jellal and Y. Zahidi, Phys. Lett. A **380**, 773 (2016).
- [40] A. Jellal, A. D. Alhaidari and H. Bahlouli, Phys. Rev. A **80**, 012109 (2009).
- [41] H. Bahlouli, A. Jellal and Y. Zahidi, Int. J. Geom. Meth. Mod. Phys. **11**, 1450036 (2014).
- [42] M. J. Bueno, J. Lemos de Mello, C. Furtado and A. M. de M. Carvalho, Eur. Phys. J. P **129**, 201 (2014).
- [43] A. Boumali and H. Hassanabadi, Eur. Phys. J. Plus **128**, 124 (2013).
- [44] J. Amaro Neto, M. J. Bueno and C. Furtado, Annals of Physics (2016).
- [45] C. Furtado *et al.*, Phys. Lett. A **195**, 90 (1994).
- [46] P. E. Lammert, V. H. Crespi, Phys. Rev. Lett. **85**, 5190 (2000).
- [47] A. Cortijo and M. A. H. Vozmediano, EPL **77**, 47002 (2007).
- [48] C. Furtado, F. Moraes and A. M. de M. Carvalho, Phys. Lett. A **372**, 5368 (2008).
- [49] J. K. Pachos, Contemporary Physics **50**, 375 (2009).
- [50] P. E. Lammert and V. H. Crespi, Phys. Rev. B **69**, 035406 (2004).
- [51] Y Aharonov and D. Bohm, Phys Rev. **115** 485 (1959).
- [52] A. Cortijo and M. A. H. Vozmediano, Nucl. Phys. B **763**, 293 (2007).
- [53] C. Furtado, A. Rosas and S. Azevedo, EPL **79** 57001 (2001).
- [54] L. Dantas and C. Furtado, Phys. Lett. A **377** 2926 (2013).
- [55] A. Rüegg, C. Lin Phys. Rev. Lett. **110**, 046401 (2013)
- [56] B. Chakraborty, K. S Gupta and S. Sen, J Phys A: Math. Theor. , **46** 055303 (2013).
- [57] V. M. Villalba, Phys. Rev. A **49**, 586 (1994).
- [58] M. Buttiker, Y. Imry, and R. Landauer, Phys. Lett. **96A**, 365 (1983).
- [59] V. Chandrasekhar, R. A. Webb, M. J. Brady, M. B. Ketchen, W. J. Gallagher, and A. Kleinsasser, Phys. Rev. Lett. **67**, 3578 (1991).
- [60] H. Bluhm, N. C. Koshnick, J. A. Bert, M. E. Huber, and K. A. Moler, Phys. Rev. Lett. **102**, 136802 (2009).

- [61] A. C. Bleszynski, W. E. Shanks, B. Peaudecerf, E. Ginossar, F. von Oppen, L. Gralman, and J. G. E. Harris, *Science* **326**, 272 (2009).
- [62] D. Mailly, C. Chapelier, and A. Benoit, *Phys. Rev. Lett* **70**, 2020 (1993).
- [63] N. Byers, C. N. Yang, *Phys. Rev. Lett.* **7**, 46 (1961).
- [64] K. Bakke, C. Furtado and S. Sergeenkov, *Europhys. Lett.* **87**, 30002 (2009).
- [65] K. Bakke and C. Furtado, *Quantum Inf. Comput.* **11**, 4444 (2011).
- [66] K. Bakke and C. Furtado, *Quantum Inf. Process* (2012), DOI: 10.1007/s 11128-012-0358-4.
- [67] L. Dantas, C. Furtado and A. L. Silva Netto, *Phys. Lett. A* **379** 11 (2015).